Modelling Globular Clusters as Multi-wavelength Emitters

Hambeleleni Davids[⋆,a,b], Christo Venter[b], Michael Backes[a]

[a] Department of Physics, Chemistry & Material Science, University of Namibia
[b]Centre for Space Research, North-West University

Eighth HEASA Conference
Virtual, Potchefstroom

September 2021

Globular clusters

- $\sim$ 160 Galactic globular clusters (GCs) in our Galaxy (Harris 1996)
- $< r > \sim 10\,\mathrm{kpc}$
- GCs contain $\sim 10^6$ old and low-mass stars
- High-density core: large stellar interaction rate
- Millisecond pulsars (MSPs), cataclysmic variables (CVs), low-mass X-ray binaries (LMXBs)

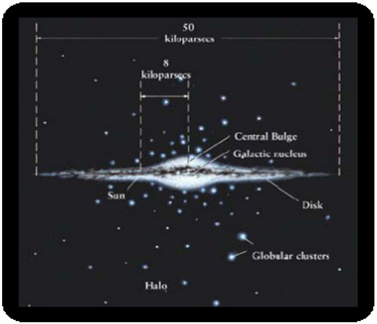

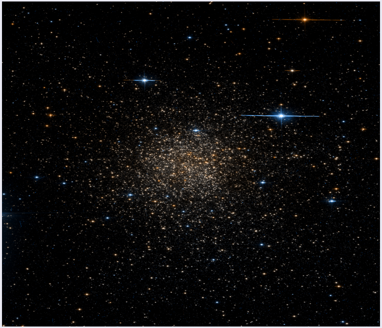

Motivation

- Study GC visibility for H.E.S.S.
- Constrain the model with H.E.S.S. upper limits
- Gather more data on Terzan 5: Fit the broadband spectral energy distribution using a leptonic model
- Derive constraints on the MSP luminosity function using the diffuse X-ray data and the *Chandra* sensitivity
- Demonstrate that uncertainty in model parameters leads to a large spread in the predicted flux: H.E.S.S. GC population, M15 and Omega Cen

Terzan 5

- Terzan 5 was discovered in the 1960s, located at a distance $d = 5.9 \pm 0.5\,\mathrm{kpc}$ (Valenti et al. 2007)
- High central stellar density and metallicity.
- Highest stellar interaction rate (Verbunt & Hut 1987)
- Hosts the largest number of MSPs (39)
- Only GC plausibly detected at very-high energies (Abramowski et al. 2011)

Previous Radio Observations of Terzan 5

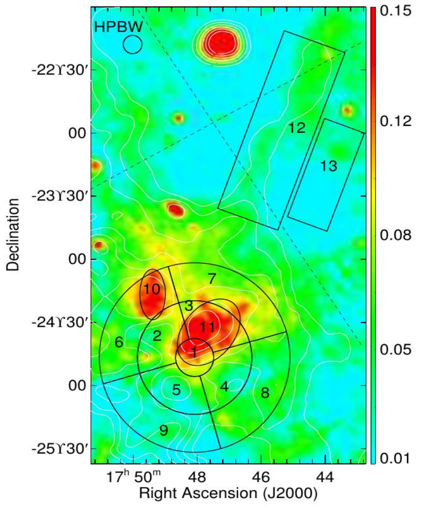

- Terzan 5 was detected in the NRAO VLA Sky Survey (NVSS) at 21 cm as a single source with a flux of 5 mJy (Condon et al. 1998)
- Several radio structures were detected in the direction of Terzan 5 (Clapson et al. 2011)
- We fit the radio data using a diffuse Low-energy synchrotron radiation component

Diffuse X-ray Emission

- Discovery of hard and diffuse X-ray emission (Eger et al. 2010)
- The diffuse X-ray signal was found to be extended well beyond the R_h of the GC
- The surface brightness peaks near the centre and decreases smoothly outwards

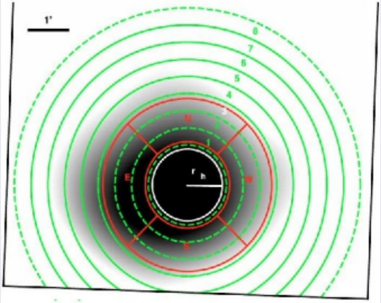

High Energy: New *Fermi* Data Analysis:

- Second GC to be associated with *Fermi* LAT source (Abdo et al. 2010; Kong et al. 2010; Nolan et al. 2012)
- Total number of MSPs in Terzan 5 estimated to be 180^{+100}_{-90} (Abdo et al. 2010)
- We selected 7 years of Pass 8 (P8) LAT data (Atwood et al. 2013) and the new *Fermi* data proved constraining for the low-energy tail of the unpulsed inverse compton component

Very-High-Energy Emission (VHE): H.E.S.S. Data

- VHE γ-ray source in the direction of Terzan 5. No new observations have been carried out on this source since its discovery (Abramowski et al. 2011)

M15

- Total stellar luminosity $7 \times 10^5 L_{\rm sun}$
- Core radius $0.43\,\rm pc$, half-mass radius $3.04\,\rm pc$
- Distance $10.4\,\rm kpc$ (Harris 1996)
- Eight MSPs (Freire et al. 2015)
- MAGIC observations: $165\,\rm h$
- Deep limit $F(>300\,\rm GeV) < 3.2 \times 10^{-13}\,\rm cm^{-2}s^{-1}$, $< 0.26\%$ of the Crab Nebula flux

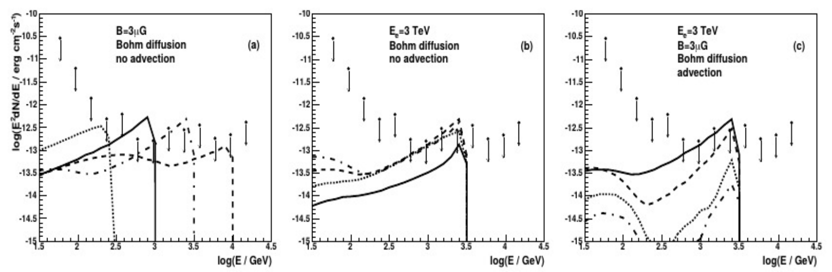

Omega Cen

- Distance: $5\,\mathrm{kpc}$, mass: $4 \times 10^6 M_{\mathrm{sun}}$, age: $11.5\,\mathrm{Gyr}$
- Brightest GC, visible to naked eye
- Most massive GC in Milky Way, may contain black hole
- May be the core remnant of disrupted dwarf galaxy
- 5 new radio pulsars detected (Dai et al., 2020)

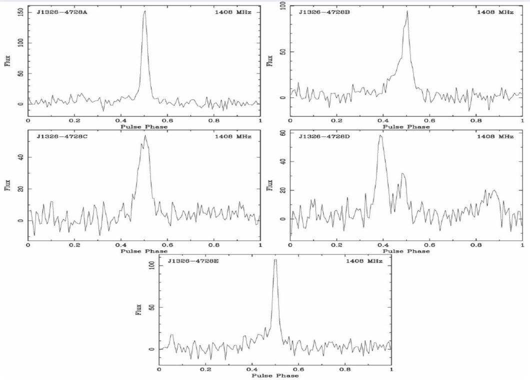

Various Models

- Pulsars
  - Magnetospheric leptonic (pulsed emission): Bednarek & Sitarek (2007); Venter et al. (2008), (2009); Cheng et al. (2010); Zajczyk et al. (2013); Bednarek et al. (2016)
  - Cluster leptonic (unpulsed emission): Bednarek & Sitarek (2007); Kopp et al. (2013); Bednarek et al. (2016); Ndiyavala et al. (2018), (2019), (2021)
- White dwarfs (Bednarek 2012)
- Hadronic (Domainko 2011)
- Dark Matter (Brown et al 2018)

Spectral components expected from GC MSPs

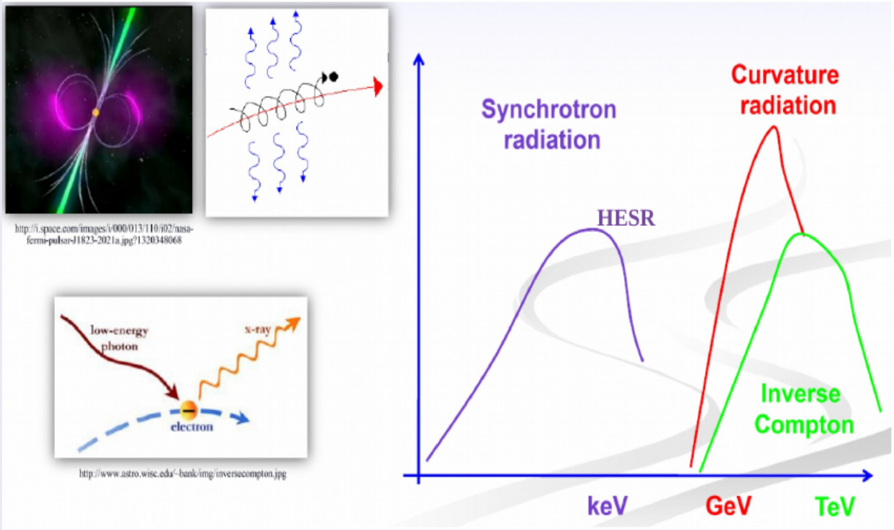

I. GC Model (Kopp et al. 2013 Model)

- multi-zone, steady-state, spherically symmetric model
- assumes pulsars to be the sources of relativistic leptons in the GCs

$$\frac{\partial n_{\mathrm{e}}}{\partial t} = \vec{\nabla} \cdot \left(\mathcal{K} \cdot \vec{\nabla} n_{\mathrm{e}} \right) - \frac{\partial}{\partial E_{\mathrm{e}}} \left(\dot{E}_{\mathrm{e}} n_{\mathrm{e}} \right) + Q$$

$\mathcal{K}$	spatial diffusion tensor
n_{e}	electron density per energy and volume
E_{e}	electron energy
$\dot{E}_{\mathrm{e}}$	radiation losses
Q	source term for the electron density in $(\mathrm{erg\ s\ cm}^3)^{-1}$

- predict the spectral energy distribution from GCs for a very broad energy range by considering synchrotron radiation (SR), as well as IC losses and diffusion

II. Leptonic Pulsar Model (Harding and Kalapotharakos 2015)

- Model of pulsed high-energy radiation over the entire spectrum from optical to VHE γ-ray wavelengths
- Pairs radiate SR in the outer magnetosphere; they originate from PC cascades
- Primary particles radiate CR; they are accelerated by an electric field
- $P = 7.7\,\mathrm{ms}$
- $\dot{P} = (6.4 \times 10^{19} I_{45})^{-2}(\frac{B^2}{P})$, where $I_{45} = \frac{I}{10^{45}\,\mathrm{g\,cm^2}}$ is the moment of inertia
- Constant electric field

Parameter Study

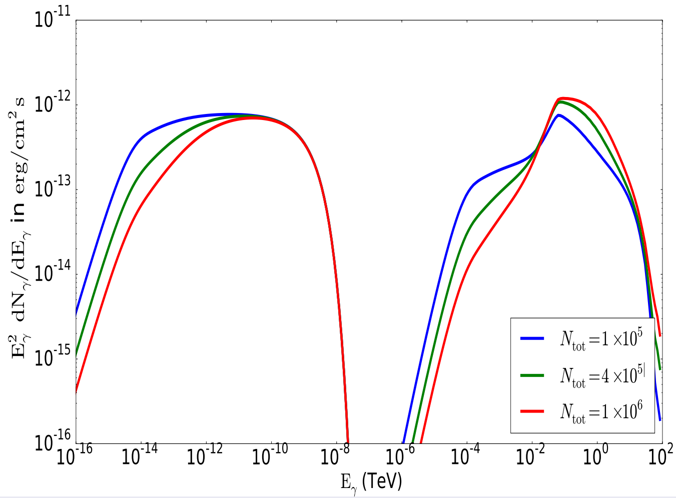

Parameter Study Cont.....

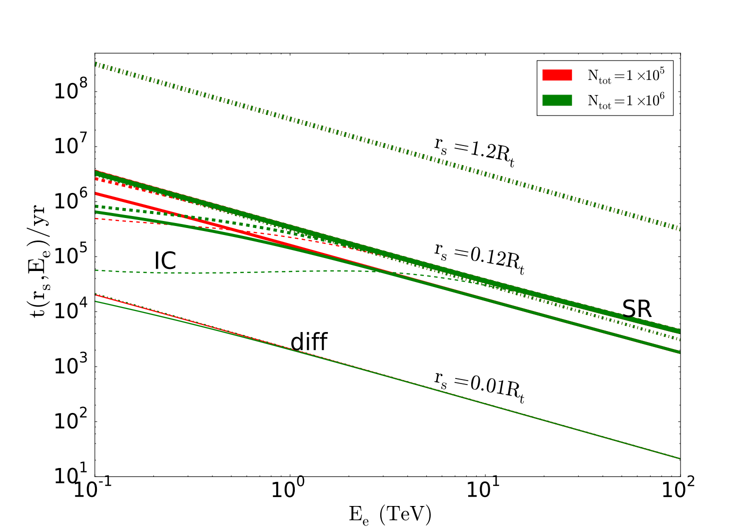

Parameter Study Cont.....

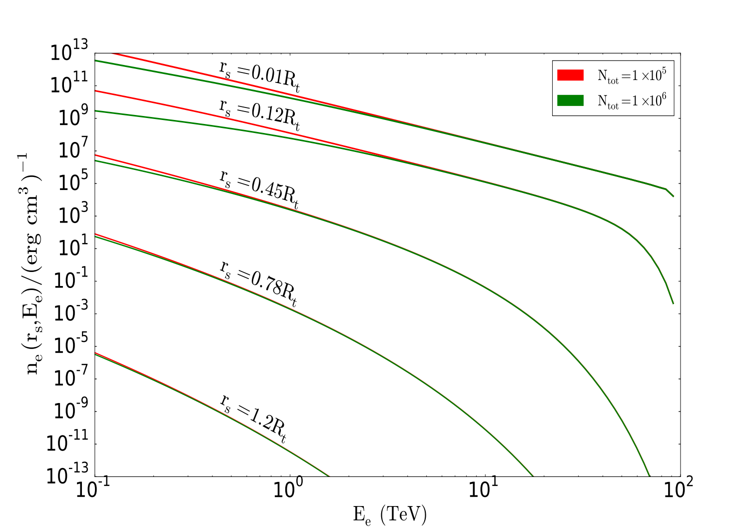

H.E.S.S. Upper Limit: 15 GCs

- H.E.S.S. searched for TeV emission from 15 GCs (Abramowski et al. 2013)
- Total exposure: 195 h of good quality data
- Results: No significant excess emission was seen above the estimated background for any of the 15 selected GCs

GC name	E_{th} (TeV)	N_{ON} (counts)	N_{OFF} (counts)	$\frac{1}{\alpha}$	Sig (σ)	$F_{\mathrm{UL}}(E > E_{\mathrm{th}})$ $\times 10^{-12}$ (ph cm^{-2}s^{-1})	livetime (h)
(i) standard cuts							
NGC 104	0.72	72	941	18.2	2.6	1.9	23.1
NGC 6388	0.28	180	2365	14.9	1.6	1.5	17.9
NGC7078	0.40	119	1988	15.0	-1.2	0.72	12.3
Terzan 6	0.28	202	8194	42.0	0.5	2.1	15.2
Terzan 10	0.23	76	2455	36.0	0.9	2.9	4.2
NGC 6715	0.19	159	2361	15.2	0.3	0.93	11.8
NGC 362	0.59	18	533	33.0	0.4	2.4	5.0
Pal 6	0.23	363	10810	31.4	1.0	1.2	24.7
NGC 6256	0.23	64	1869	27.4	-0.5	3.2	5.3
Djorg 2	0.28	56	2387	39.4	-0.6	0.84	4.6
NGC 6749	0.19	84	2633	29.3	-0.6	1.4	8.2
NGC 6144	0.23	63	2196	30.8	-1.0	1.4	4.7
NGC 288	0.16	647	24148	38.5	0.8	0.53	46.7
HP 1	0.23	67	2771	34.3	-1.6	1.5	5.6
Terzan 9	0.33	89	2556	31.7	0.9	4.5	5.2
Stacking analysis							
-	0.23	2242	67826	31.2	1.6	0.33	195

- Detection of Terzan 5 with 5.3σ (Abramowski 2011)

Top 5 promising candidates: (for best-guess model parameters)

- NGC 6388, 47 Tucanae (NGC 104), Terzan 5, Djorg 2, and Terzan 10

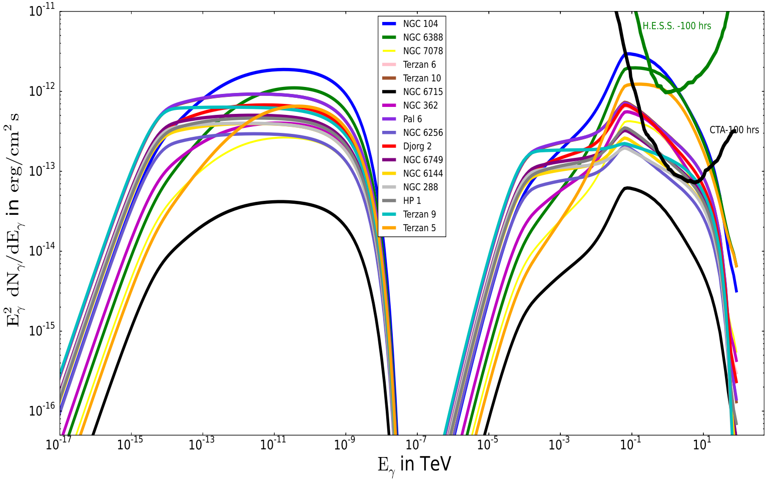

Constraining Parameters

Terzan 5:

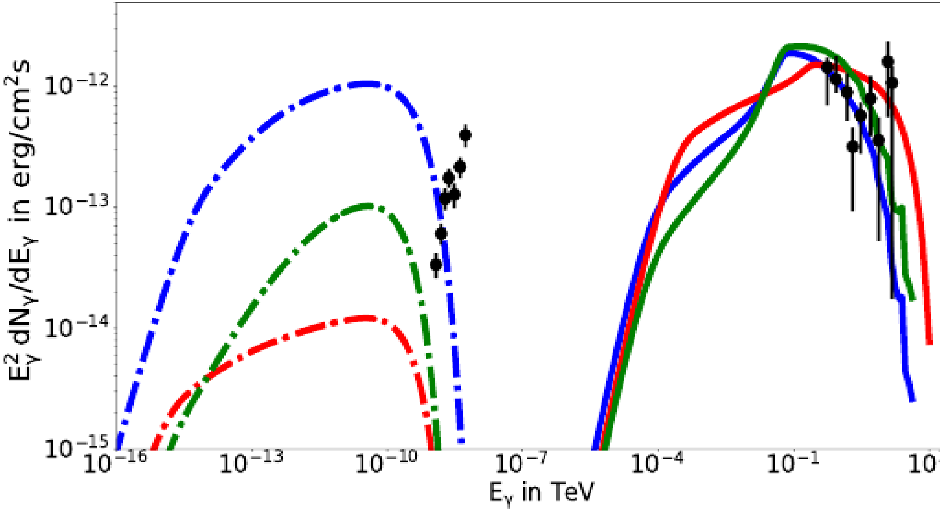

Optical Upper Limit

- Our leptonic model predicts diffuse SR at low level (Kopp et al. 2013; Ndiyavala et al. 2019).
- Very difficult to directly observe this component because of $\sim 10^5$ stars that contribute a high level of blackbody radiation.
- Obtain the BB flux from stars in different annuli (Trager et al. 1995).
- We estimate the thermal flux level:

$$\begin{aligned}\frac{B_\nu <\nu> A_\star}{d^2} &= \frac{8\pi R_\star^2 h <\nu>^4 N_{\rm ann}}{d^2 c^2}\frac{1}{e^{\frac{h\nu}{k_B T}}-1}\\ &\sim 1.7\times 10^{-14} R_{\star,10}^2 N_{\rm ann}\,{\rm erg\,cm^{-2}s^{-1}}\end{aligned}$$

  assuming $R_{\star,10} = R_\star/10^{10}\,{\rm cm}$ and $d = 5.9\,{\rm kpc}$.
- Expected BB flux is $\sim 10^5$ times higher than expected SR flux for full GC.

Broadband SED of Terzan 5

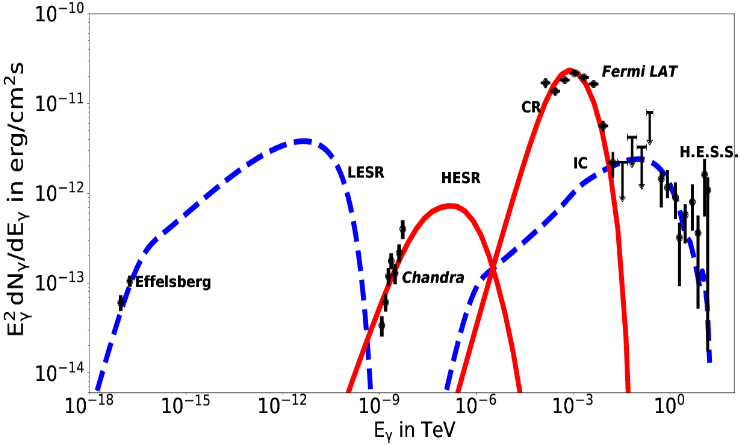

Constraining the Pair Multiplicity Spatial Distribution of the Pulsar Population

- **Unpulsed SR:**

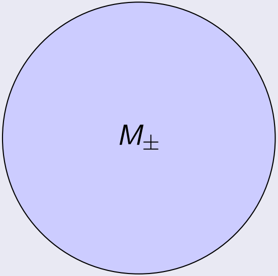

- $M_{\mathrm{avg}} = 158$ for the Kopp et al. 2013 and $M_{\mathrm{avg}} = 2.9 \times 10^4$ for the Harding and Kalapotharakos 2015.

- **Pulsed SR:** Split M into $M_{\mathrm{vis}}, M_{\mathrm{invs}}, M_{\mathrm{avg}}$

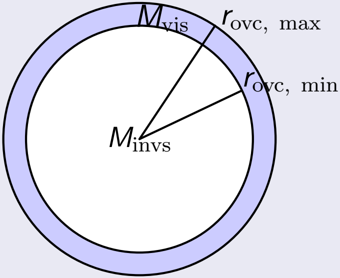

- $M_{\mathrm{vis}} = 2.5 \times 10^3$, $M_{\mathrm{invis}} = 115$, $M_{\mathrm{avg}} = 158 \Rightarrow$ Consistency.

Updated Broadband SED of Terzan 5

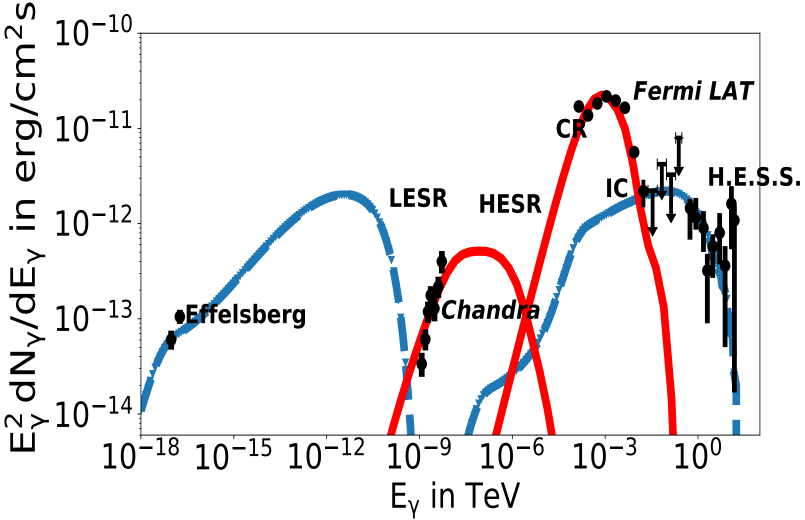

MSP Population Energetics

- **First approach:** degenerate, but reasonable parameters.
- **Second approach:** We modeled the underlying (visible and invisible) pulsar population via a parametric spin-down luminosity function $dN/d\dot{E} = N_0(\dot{E}/\dot{E}_0)^{-(1+\gamma)}$ (Johnston & Verbunt 1996).
- Balance of energetics: using the observed and estimated unobserved non-thermal X-ray luminosity (Eger et al. 2010) & the *Chandra* point-source detection sensitivity.

$$L_{\mathrm{X,vis}} = \eta^{\mathrm{X}}_{\mathrm{vis}} N^{\mathrm{X}}_{\mathrm{vis}} \langle \dot{E} \rangle_{\mathrm{vis}}$$
$$L_{\mathrm{X,invis}} = \eta^{\mathrm{X}}_{\mathrm{invis}} N^{\mathrm{X}}_{\mathrm{invis}} \langle \dot{E} \rangle_{\mathrm{invis}}$$

$$N^{\mathrm{X}}_{\mathrm{tot}} = \int_{\dot{E}_{\mathrm{min}}}^{\dot{E}_{\mathrm{max}}} \left(\frac{dN}{d\dot{E}} \right) d\dot{E},$$

$$N^{\mathrm{X}}_{\mathrm{vis}} = \int_{\dot{E}_{\mathrm{b}}}^{\dot{E}_{\mathrm{max}}} \left(\frac{dN}{d\dot{E}} \right) d\dot{E},$$

$$N^{\mathrm{X}}_{\mathrm{invis}} = \int_{\dot{E}_{\mathrm{min}}}^{\dot{E}_{\mathrm{b}}} \left(\frac{dN}{d\dot{E}} \right) d\dot{E},$$

$$\langle \dot{E} \rangle_{\mathrm{vis}} = \frac{1}{N^{\mathrm{X}}_{\mathrm{vis}}} \int_{\dot{E}_{\mathrm{b}}}^{\dot{E}_{\mathrm{max}}} \dot{E} \left(\frac{dN}{d\dot{E}} \right) d\dot{E}$$

$$\langle \dot{E} \rangle_{\mathrm{invis}} = \frac{1}{N^{\mathrm{X}}_{\mathrm{invis}}} \int_{\dot{E}_{\mathrm{min}}}^{\dot{E}_{\mathrm{b}}} \dot{E} \left(\frac{dN}{d\dot{E}} \right) d\dot{E}$$

Table 2. Sample parameter combinations that lead to a balance of the X-ray-implied energetics.

η_X	$\dot{E}_{\rm invis}$	$\dot{E}_{\rm vis}$	$\dot{E}_{\rm min}$	$\dot{E}_{\rm max}$	γ_L	$N_{\rm vis}^X$	$N_{\rm invis}^X$	$N_{\rm tot}^X$
0.05%	3×10^{33}	9.2×10^{34}	10^{31}	2.4×10^{35}	−0.19	43	45	88
0.05%	3.5×10^{32}	1.8×10^{35}	10^{29}	10^{36}	0.21	22	399	421
0.5%	1.2×10^{32}	3.8×10^{34}	10^{31}	10^{36}	0.5	10	116	126
0.5%	1.5×10^{32}	2.8×10^{34}	10^{31}	3.6×10^{35}	0.4	14	96	110
1%	7.4×10^{31}	2.5×10^{34}	10^{31}	2.0×10^{36}	0.6	8	95	103
1%	1.3×10^{32}	2.4×10^{34}	3.0×10^{31}	2.9×10^{36}	0.64	8	53	61
1%	2.5×10^{32}	2×10^{34}	10^{32}	3×10^{36}	0.685	10	27	37

NOTE—The units of the spin-down luminosities are erg s^{-1}.

- Very coupled system. A different choice of η_x (or $\langle \dot{E} \rangle_{\rm vis}$) will lead to a different solution.
- Future constraints on, e.g.,$N_{\rm vis}$ and $\langle \dot{E} \rangle_{\rm vis}$ may lead to better constraints on these parameters plus the pair multiplicity $M_{\pm}$.

Estimating Uncertainties in the Predicted Gamma-ray Flux of Globular Clusters in the Cherenkov Telescope Array Era

Convergence

- Finer sampling of parameter space (Ndiyavala-Davids et al. 2021)

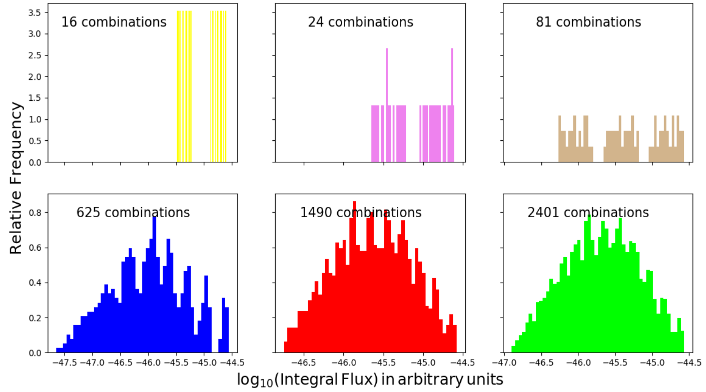

Convergence

- More trials: parameter combinations (Ndiyavala-Davids et al. 2021)

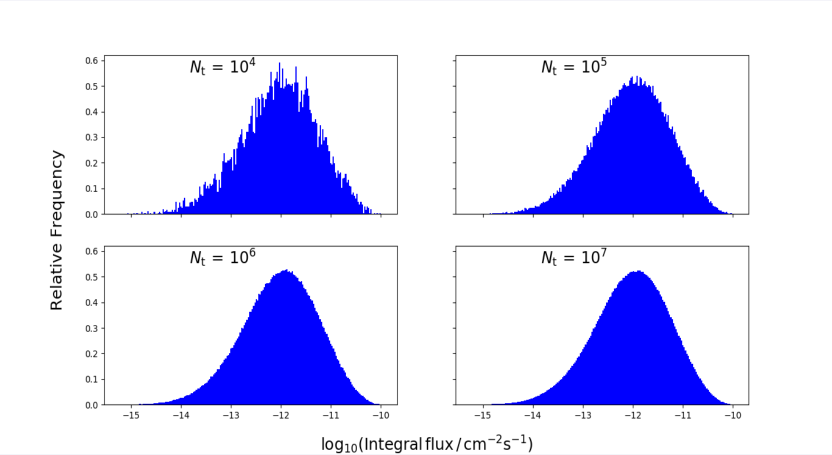

GC Population

- First and second parameter combinations (Ndiyavala-Davids et al. 2021)

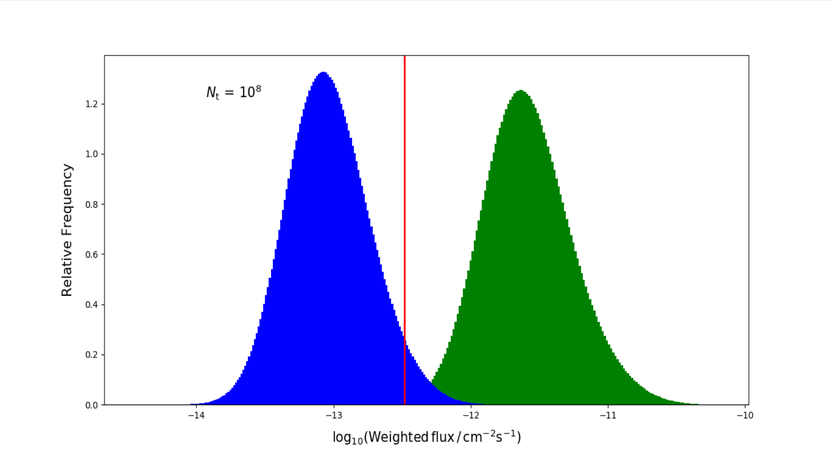

- Two parameter range combinations (second: lower source term; Ndiyavala-Davids et al. 2021)

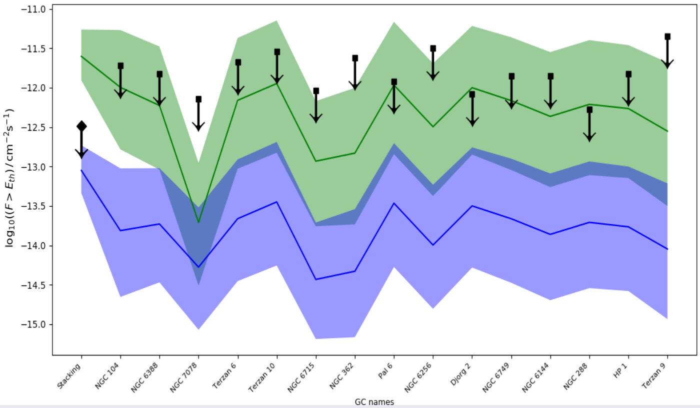

M15

- Magic differential upper limits; Ndiyavala-Davids et al. 2021)

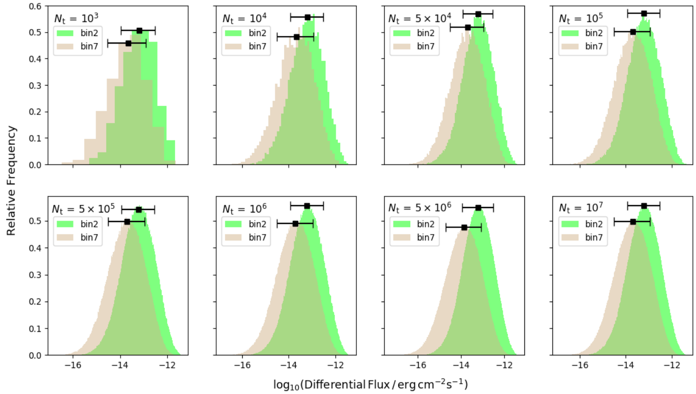

M15

- Median + uncertainty band: due to uncertain model parameters
- Example model predictions (Ndiyavala-Davids et al. 2021)

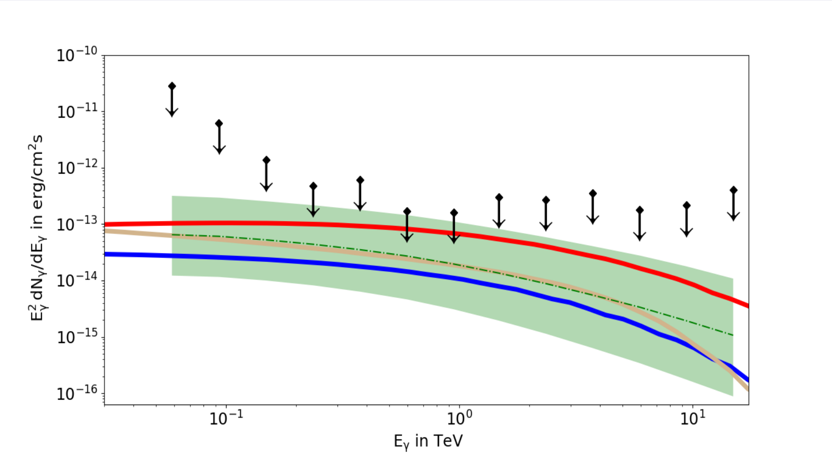

Omega Cen

- Median + uncertainty band: due to uncertain model parameters
- Example model predictions (Ndiyavala-Davids et al. 2021)

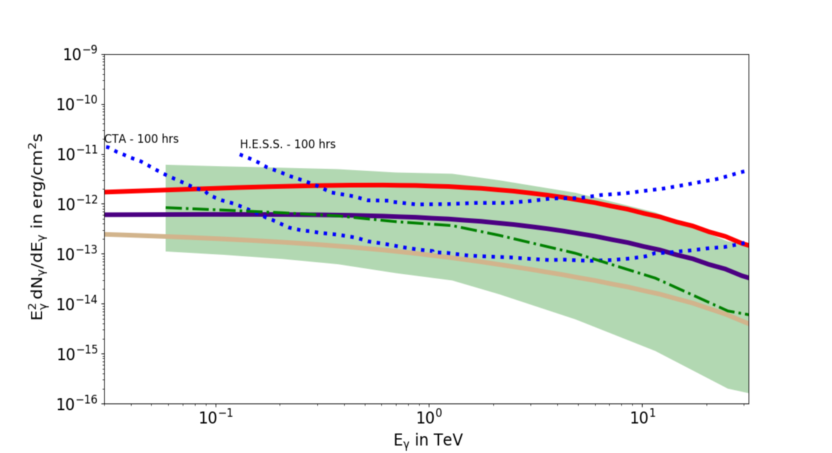

Conclusions

- Flux predictions and performed a parameter study, varying six model parameters
- Parameters of the individual GCs were uncertain and quite unconstrained by the available data: $B, \Gamma, N_{\star}, d, \kappa, Q_0$
- H.E.S.S. may detect two more GCs if they observe these sources for ~ 100 hours
- Fit the radio spectral points by invoking an LESR component that might extend into the optical range and X-rays using HESR component
- Energetics and numbers of the MSP source population needed to reproduce the detected diffuse X-ray emission are plausible
- Assessed uncertainties in the predicted VHE γ-ray flux of GCs and gave theoretical guidance to CTA's observational strategy

Thank You!